

The Role of Odd-Electron Intermediates and In-Cage Electron Transfer in Ultrafast Photochemical Disproportionation Reactions in Lewis Bases

Matthias F. Kling, James F. Cahoon, Elizabeth A. Glascoe, Jennifer E. Shanoski, and Charles B. Harris*

Department of Chemistry, University of California, Berkeley, California 94720, and Chemical Sciences Division, Lawrence Berkeley National Laboratory, Berkeley, California 94720

Received June 25, 2004; E-mail: harris@socrates.berkeley.edu

The $18e^-/16e^-$ rule is well established in organometallic chemistry. It predicts greater stability for complexes with closed-shell configurations. Although even-electron intermediates dominate a variety of transition metal reactions, the importance of odd-electron (open-shell) species in catalysis has long been recognized.¹ The photochemical disproportionation of metal–metal bound carbonyl dimers was reported to involve odd-electron radical intermediates.^{2–4} While $17e^-$ radicals have been observed in the homolysis of $Cp_2M_2(CO)_6$ complexes ($Cp = C_5H_5$, $M = Cr, Mo, W$),⁴ a possible 19 (or $18 + \delta$)-electron intermediate was postulated to explain disproportionation in the presence of strong Lewis bases.³ Femtosecond infrared spectroscopy is a powerful technique for studies on the mechanisms of organometallic reactions and has recently revealed the mechanism of one-electron oxidative addition in the photochemistry of the rhenium dimer $Re_2(CO)_{10}$ and identified the key intermediate as a weakly solvated $17e^-$ species.⁵

In this Communication, we report on femtosecond visible pump–IR probe studies of the photochemical disproportionation of $Cp_2W_2(CO)_6$ in 1:4 molar solutions of $P(OMe)_3$ and CH_2Cl_2 . The reaction is initiated by a laser pulse at 400 nm, and transient intermediates and photoproducts are observed on a picosecond time scale by their particular IR absorptions.⁶ In this manner, the mechanism of photoinduced disproportionation of a transition metal dimer and the importance of odd-electron species are directly addressed for the first time. The experiments are accompanied by density functional theory (DFT) calculations on the geometries, frequencies, and energetics of relevant intermediates and photoproducts.⁷ Figure 1 shows transient difference spectra recorded after 400 nm photolysis of $Cp_2W_2(CO)_6$ in a 1:4 molar solution of $P(OMe)_3$ and CH_2Cl_2 (“phosphite solution”). Two strong parent bleaches (A) are observed at 1909 and 1956 cm^{-1} originating from the $2B_u$ and A_u carbonyl stretching modes of *anti*- $Cp_2W_2(CO)_6$ (C_{2h} symmetry), the most stable isomer in nonpolar and weakly polar solutions.⁸ A negligible contribution from the *gauche* isomer is seen by its very weak bleach at 2012 cm^{-1} . Photolysis at 400 nm in neat CH_2Cl_2 and in phosphite solution primarily results in formation of monomeric $CpW(CO)_3$ radicals (B) with transient absorptions at 1880 and 1995 cm^{-1} (transient difference spectra in neat CH_2Cl_2 solutions were taken for comparison and are contained in the Supporting Information). While evidence for a carbonyl-loss pathway was found with shorter excitation wavelengths in matrices,^{9,10} no transient absorption due to $Cp_2W_2(CO)_5$ is found in phosphite solution. A carbonyl-loss species, which should have a low quantum yield at 400 nm excitation,¹¹ is expected to immediately coordinate with a phosphite and not contribute to disproportionation in a single-photon process.¹¹

In neat CH_2Cl_2 , $17e^-$ radicals (B) exhibit geminate recombination, leading to a decay of 5% within 50 ps, but show no further decay on longer time scales. In phosphite solution, however,

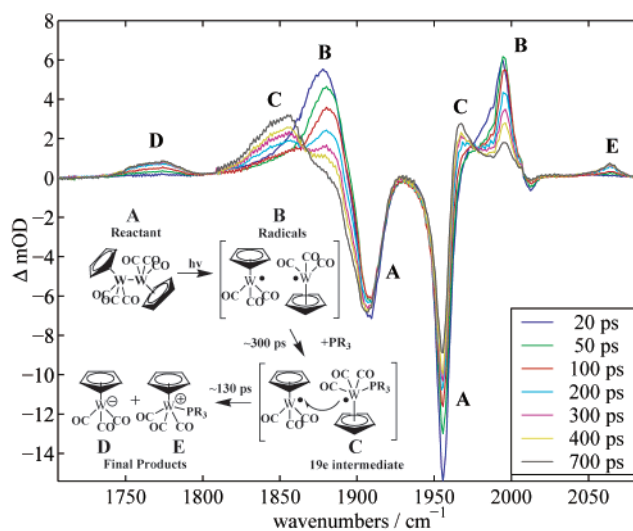


Figure 1. Transient difference spectra in the CO stretching region for $Cp_2W_2(CO)_6$ in a 1:4 molar solution of $P(OMe)_3$ and CH_2Cl_2 after photolysis at 400 nm. Species associated with peaks in the spectra and the reaction mechanisms are addressed in the inset.

complete decay of the radical (B) is observed. The chemistry in these solutions is more complex, displaying additional decay channels for $17e^-$ radicals. Four additional peaks can be seen, centered at 1770 , 1850 , 1967 , and 2064 cm^{-1} in Figure 1, that are assigned to the anionic disproportionated product $CpW(CO)_3^-$ (D), two peaks of the $19e^-$ intermediate $CpW(CO)_3P(OMe)_3$ (C), and the cationic disproportionated product $CpW(CO)_3P(OMe)_3^+$ (E), respectively.¹² Assignments are based on literature data^{8,10} and DFT calculations (see Table 1). Note that the $16e^-$ species $CpW(CO)_3^+$ is not observed on the time scale of the experiment (800 ps). To the best of our knowledge, the formation of a $19e^-$ intermediate on a picosecond time scale is monitored here for the first time. Neglecting the spectral trace at 20 ps, which shows effects of peak broadening due to vibrational excitation after photolysis, isosbestic points at 1865 and 1978 cm^{-1} in Figure 1 indicate a correlation between the radical (B) decay and $19e^-$ intermediate (C) formation. In agreement, exponential fits to kinetic data yield time constants ($\tau = k^{-1}$) of 285 ± 29 and $306 \pm 106\text{ ps}$ for the decay of radicals and formation of $19e^-$ intermediates, respectively.¹³ The formation of the $19e^-$ intermediate thus seems to be the dominant decay pathway for $CpW(CO)_3$ radicals on the hundreds of picoseconds time scale.

At first glance, ultrafast formation of two ionic disproportionation products is surprising. The accepted reaction mechanism originally suggested by Tyler³ required a $19e^-$ intermediate to collide with a parent molecule in order to transfer an electron and form the corresponding cation and negatively charged parent molecule. The

Table 1. Calculated and Observed Frequencies (cm⁻¹) of Relevant Species^a

	calculated	observed
(A) <i>anti</i> -Cp ₂ W ₂ (CO) ₆	1915.1(0.2), 1924.4(0.8), 1967.7(1.0) ^a	1909(s), 1956(s)
<i>gauche</i> -Cp ₂ W ₂ (CO) ₆	1902.2(0.2), 1908.7(0.3), 1936.7(0.4), 1970.1(0.6), 2014.4(0.4) ^a	2012(w)
(B) CpW(CO) ₃ (17e ⁻)	1906.2(0.6), 1907.0(0.4), 1988.7(0.3) ^b	1880(s), 1995(s)
(C) CpW(CO) ₃ P(OMe) ₃ (19e ⁻)	1888.2(0.5), 1899.1(0.3), 1975.3(0.4) ^a	1850(s), 1967(m)
(D) CpW(CO) ₃ ⁻ (18e ⁻)	1782.9(0.7), 1783.8(0.7), 1878.6(0.4) ^b	1770(w)
(E) CpW(CO) ₃ P(OMe) ₃ ⁺ (18e ⁻)	1989.9(0.4), 2013.3(0.2), 2064.9(0.3) ^a	1995(w), 2064(w)
CpW(CO) ₃ ⁺ (16e ⁻)	2016.2(0.2), 2018.3(0.5), 2081.1(0.2) ^b	not observed

^a Calculated frequencies are corrected by 0.9614.¹⁴ ^b Basis set A.⁷ ^c Basis set C;⁷ relative intensities are given in parentheses; observed frequencies are given for phosphite solutions. Intensities: w = weak, m = medium, s = strong.

heterolysis of the latter would result in the formation of a negatively charged CpW(CO)₃⁻ species. While this reaction mechanism could explain disproportionation on diffusion-limited time scales (nanoseconds to milliseconds), allowing for encounters of 19e⁻ intermediates and parent dimers in low concentrated solutions, it seems unlikely to be the reaction mechanism at work on a picosecond time scale.

Formation time constants for the anion, CpW(CO)₃⁻ (D), and the cation, CpW(CO)₃P(OMe)₃⁺ (E), are very similar at 127 ± 13 and 134 ± 28 ps,¹³ respectively, indicating that these two species are generated in a single kinetic event. Why, however, is the disproportionation reaction faster than the formation of CpW(CO)₃P(OMe)₃ (C), the alleged 19e⁻ intermediate in the disproportionation reaction? A microscopic view of the reaction can provide an answer to this question. Initially, homolysis of the dimer yields two 17e⁻ radicals (B) that are enclosed together in a cage of solvent molecules, as depicted by the brackets in the reaction scheme in Figure 1. The solvent cage consists of CH₂Cl₂ and P(OMe)₃ molecules and allows for immediate solvation or reaction of the 17e⁻ radicals with these species. Reference data in neat CH₂-Cl₂ reveal that chlorine atom abstraction from the chlorinated solvent, as observed in CCl₄,¹⁵ does not occur. In contrast, 17e⁻ radicals coordinate with phosphites on a time scale of ca. 300 ps. The reaction is slightly exothermic, with ΔH^o(298 K) = -1.5 kcal/mol, therefore favoring a 19e⁻ over 17e⁻ configuration.¹⁶

A 19e⁻ intermediate may be formed next to a 17e⁻ radical within the solvent cage (C, see Figure 1). The close proximity of the two odd-electron species allows for almost immediate transfer of an electron to stabilize both species in even-electron configurations. At low concentrations of P(OMe)₃, this electron-transfer reaction limits the buildup of final ionic disproportionation products D and E on an ultrafast time scale.¹⁷ An electron will be transferred between the two odd-electron species as long as they are in close proximity; however, insertion of solvent molecules between 17e⁻ and 19e⁻ radicals slows down and finally prevents charge transfer. Treating the solvent as a viscous medium and using a random walk equation, $x(\tau) = (2D\tau)^{1/2}$, in neat CH₂Cl₂ with self-diffusion coefficient $D = 1.6 \times 10^{-6}$ cm²/s, a time constant of $\tau = 130$ ps corresponds to a distance $x(\tau) = 2$ Å between two particles, the length of approximately one CH₂Cl₂ molecule.¹⁸ The 130 ps time constant for ultrafast disproportionation in phosphite solution thus roughly corresponds to the time scale for insertion of one solvent molecule between the 17e⁻ and 19e⁻ species, which quenches the

electron-transfer reaction to the ion pairs. Similar time constants were reported for solvent separation of ion-pairs in back-electron-transfer reactions in solution.¹⁹

Femtosecond IR spectroscopy in combination with DFT calculations has allowed the first real-time observation and characterization of ultrafast 19e⁻ intermediate and disproportionated product formation upon the photolysis of a transition metal dimer. Ultrafast disproportionation is found to be best described by in-cage electron transfer between two odd-electron species, namely a 17e⁻ CpW(CO)₃ radical and a 19e⁻ (or 18 + δ) CpW(CO)₃P(OMe)₃ intermediate. Photolysis studies of Cp₂W₂(CO)₆ in various phosphines and phosphites currently underway in our laboratory indicate the proposed reaction mechanism to be of fundamental importance for understanding the role of odd-electron species and in-cage electron transfer in the disproportionation of transition metal dimer complexes.²⁰

Acknowledgment. The National Science Foundation is acknowledged for funding, and the Office of Basic Energy Sciences, Chemical Sciences Division, of the U.S. Department of Energy under contract DE-AC03-76SF00098 for the use of some specialized equipment. M.F.K. acknowledges support by the Alexander von Humboldt foundation through a Feodor-Lynen Fellowship.

Supporting Information Available: Details of the experimental setup, spectra obtained in CH₂Cl₂ solutions, and kinetic data. This material is available free of charge via the Internet at <http://pubs.acs.org>.

References

- (1) Baird, M. C. *Chem. Rev.* **1988**, *88*, 1217–1227. Astruc, D. *Chem. Rev.* **1988**, *88*, 1189–1216.
- (2) Tyler, D. R. *Acc. Chem. Res.* **1991**, *24*, 325–331. Stiegman, A. E.; Tyler, D. R. *Coord. Chem. Rev.* **1985**, *63*, 217–240.
- (3) Stiegman, A. E.; Stieglitz, M.; Tyler, D. R. *J. Am. Chem. Soc.* **1983**, *104*, 6032–6037.
- (4) Bitterwolf, T. E. *Coord. Chem. Rev.* **2001**, *211*, 235–254.
- (5) Yang, H.; Snee, P. T.; Kotz, K. T.; Payne, C. K.; Frei, H.; Harris, C. B. *J. Am. Chem. Soc.* **1999**, *121*, 9227–9228.
- (6) Details of the experimental setup are contained in the Supporting Information.
- (7) DFT calculations have been carried out with Gaussian98, Revision A9 (Frisch et al., Gaussian, Inc., Pittsburgh, PA, 1998) applying the B3LYP functional and generic basis sets (LANL2DZ core potential for W and 6-31G(d) (A), 6-311G(d,p) (B), and 6-311+G(d,p) (C) basis sets for other atoms).
- (8) Virrels, I. G.; George, M. W.; Johnson, F. P. A.; Turner, J. J.; Westwell, J. R. *Organometallics* **1995**, *14*, 5203–5208.
- (9) Hooker, R. H.; Rest, A. J. *J. Chem. Soc., Dalton Trans.* **1990**, 1221–1229.
- (10) Baker, M. L.; Bloyce, P. E.; Campen, A. K.; Rest, A. J. *J. Chem. Soc., Dalton Trans.* **1990**, 2825–2832.
- (11) Bitterwolf, T. E.; Saygh, A.; Shade, J. E.; Rheingold, A. L.; Yap, G. P. A.; Liable-Sands, L. *J. Organomet. Chem.* **1998**, *562*, 89–96.
- (12) Note that the radical peak at 1995 cm⁻¹ is partially overlapped with another peak of the cationic product, resulting in residual absorption at longer delay times at this wavenumber.
- (13) Errors correspond to 95% confidence intervals. The time constant for the 19e⁻ intermediate was obtained via Gaussian peak fitting, and larger errors result from spectral overlap with the radical peak.
- (14) Scott, A. P.; Radom, L. *J. Phys. Chem.* **1996**, *100*, 16502.
- (15) Scott, S. L.; Espenson, J. H.; Zhu, Z. *J. Am. Chem. Soc.* **1993**, *115*, 1789–1797.
- (16) DFT-UB3LYP/basis set B, ZPE, and thermal corrections for 298 K calculated on the same level.
- (17) Preliminary data taken at various concentrations of P(OMe)₃ revealed that the disproportionation rate is most likely limited by electron transfer at low concentrations and by 19e⁻ intermediate formation at high concentrations. Details will be discussed in ref 20.
- (18) Yu, Y.-X.; Gao, G.-H. *Fluid Phase Equil.* **1999**, *166*, 111–124.
- (19) Gould, I. R.; Farid, S. *Acc. Chem. Res.* **1996**, *29*, 522–528.
- (20) Cahoon, J. F.; et al., to be published.

JA046223X